Phys. Status Solidi A **206**, No. 6, 1240–1244 (2009) / **DOI** 10.1002/pssa.200881036

physica status solidi a
www.pss-a.com
applications and materials science

Structure and photoluminescence studies of porous silicon formed in ferric ion containing stain etchants

Margaret E. Dudley[**] **and Kurt W. Kolasinski**[*]

Department of Chemistry, West Chester University, West Chester, PA 19383 USA

Received 12 March 2008, revised 3 December 2008, accepted 8 December 2008
Published online 25 March 2009

PACS 61.43.Gt, 78.55.Mb, 78.67.Bf, 81.05.Rm, 81.07.Bc, 81.65.Cf

[*] Corresponding author: e-mail kkolasinski@wcupa.edu, Phone: +001 610 436 2968, Fax: +001 610 436 2890
[**] e-mail mdudley@ucsd.edu

Stain etching of silicon in aqueous solutions composed of $FeCl_3$ + HF + concentrated ($HClO_4$ or H_2SO_4) leads to highly luminescent porous Si with a unique dual layer structure. The upper layer (~3 µm thick) exhibits bluer luminescence (peaked at 560–590 nm) and a porosity in excess of 84%. The lower layer exhibits redder luminescence (peaked at 630–645 nm) and a lower porosity. Both layers are crystalline and are composed predominantly of uniform micropores. Because of the substantially higher porosity of the upper layer, this layer is highly susceptible to cracking and exfoliation. Critical point drying greatly reduces cracking and exfoliation but does not eliminate cracking completely. Brushing easily removes the upper layer while leaving the lower layer intact and the removed material remains photoluminescent.

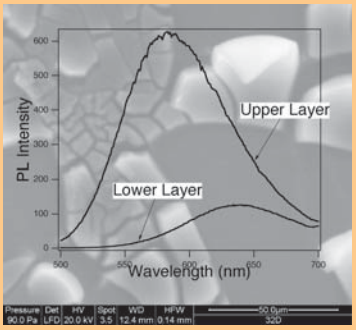

Scanning electron micrograph and photoluminescence spectrum from a stain etched film dried in air from a methanol rinse.

1 Introduction Stain etching of Si is an electroless form of por-Si formation that involves an acidic aqueous mixture of fluoride and an oxidant [1]. Nahidi and Kolasinski [2] have previously shown the ferric ion Fe^{3+} introduced as a chloride can be effectively used as the oxidant. An attractive feature of these solutions is that bubble formation is suppressed compared to a typical stain etchant such as HF + HNO_3. This helps to make these films structurally and optically (at least in terms of PL intensity and color) more uniform. However, these solutions, especially those formed from NH_4HF_2 + HCl + $FeCl_3$ and HF + $FeCl_3$ exhibit a substantial induction period before the initiation of por-Si formation. The induction period leads to great variability in the results of etching when etching times are short.

The role of the oxidant is to inject holes into the Si valence band [3]. The oxidant must have a sufficiently positive electrochemical potential to enable hole injection. The Fe^{3+} ion with E_0 = +0.77 V has an E_0 value close to the limiting smallest positive value. Therefore, we expect that only oxidants equally or more positive than Fe^{3+} can be useful in stain etchants. Solution composition also affects the electrochemical potential of an ion, which is determined by the activity according to the Nernst equation, and the position of the Si valence band maximum responds to solution composition particularly if hydrogen or fluoride ions are able to diffuse into the space charge layer. We have sought to optimize stain etchants using Fe^{3+} and to determine how film properties respond to solution composition by investigating a number of new formulations of stain etchants.

2 Experimental All samples were etched from Si(100), Czochralski grown, B doped, p-type prime grade

wafers with 14–22 Ω cm resistivity and 500–550 μm thickness. All solutions were aqueous and all etching was performed at room temperature. A number of oxidants have been used, including the addition of Fe^{3+} as $FeCl_3$ and $Fe(NO_3)_3$, ($E_0(NO_3^-) = +0.96$ V), Ce^{4+}($E_0 = 1.61$ V as cerium ammonium sulfate) and the addition of $HClO_4$ ($E_0(ClO_4^-) = 1.23$ V), H_2SO_4, H_3PO_4, HCl and HNO_3. Fluoride is supplied either from HF or NH_4HF_2. Several surfactants have also been added to these solutions including alcohols and neutral, anionic and cationic surfactants. None of the surfactants have been found to produce satisfactory results. For any of the myriad combinations that we have tried, suppression of bubble formation was always accompanied by the slowing of porous film formation to the point where the solutions were no longer practicable stain etchants, at least for the thick (>1 μm) layers that we are attempting to produce.

After etching the samples are rinsed several times, first in water then methanol or ethanol. Critical point drying is performed in a Tousimis AutoSamDri 815 critical point drier with ethanol as the initial liquid solvent being replaced by a supercritical fluid of ethanol and CO_2.

Scanning electron microscopy (SEM) was performed with an FEI Quanta 400 ESEM, at a voltage of 5–15 kV with a working distance of 10–15 mm. The highly porous upper layer exhibits strong charging effects; therefore imaging was generally performed in a background of ~100 Pa of water in an environmental SEM mode. The SEM operates with integrated Oxford INCA energy dispersive X-ray spectroscopy (EDS). Imaging and selective area diffraction were performed with an FEI Tecnai T12T transmission electron microscope (TEM) operating at 120 kV.

Photoluminescence (PL) and PL excitation (PLE) spectroscopies were performed on a Cary Eclipse Fluorescence spectrometer, with slit widths set for 5 nm resolution and filtering on both the emission and excitation. While PL spectra were observed to change over the course of several hours, they do not change over the course of the time scale of a minute or so required to acquire a single spectrum.

3 Results and discussion

3.1 Etchant composition Ce^{4+} precipitates as CeF_4 when added to HF. Nonetheless when a Si crystal is placed in contact with the wet CeF_4 precipitate, a photoluminescent por-Si layer is formed. We have found that precipitated CeF_4 can be dissolved by the presence of a strong acid, such as H_2SO_4. A sufficient Ce^{4+} concentration can be achieved to facilitate stain etching. Porous layers formed from the Ce^{4+} ion retain a brilliant photoluminescence over a period of months.

We expected $HClO_4$ + HF solutions to act as stain etchants. We observed clear signs of etching but have yet to find a composition that leads to por-Si formation. Neither H_2SO_4 nor H_3PO_4 + HF led to etching or por-Si formation because H_2SO_4 and H_3PO_4 cannot inject holes into Si. As is well known, HNO_3 + HF leads to por-Si formation but only with production of copious bubbles [1, 4]. The use of $Fe(NO_3)_3$ + HF leads to vigorous etching of Si. One can easily create an etchant that will consume a 1 cm^2, 500 μm thick wafer in a matter of a few minutes. This etchant also produces copious bubbles. To produce a stain etchant requires a very low concentration of the ferric nitrate.

The most promising new stain etchants were produced by adding $FeCl_3$ + HF + either $HClO_4$ or H_2SO_4. $HClO_4$ is able to inject holes into the Si valence band, but also it can oxidize Fe^{2+} to reform Fe^{3+}. A range of composition exhibits the formation of photoluminescent por-Si. We have not fully explored the composition ranges to determine all possible compositions that serve to produce por-Si. We have concentrated on the solutions produced by using a total volume of 10 ml to which was added 1.2–1.7 g ferric chloride hexahydrate. The liquid added to the solution is a mixture of 48% HF + 11 M $HClO_4$ or 18 M H_2SO_4. The ratio of HF to acid ranged from 1 : 9 to 10 : 0.

3.2 Structural studies The $FeCl_3$ + HF + $HClO_4$ or H_2SO_4 stain etchants produced a por-Si layer unlike any we have previously observed [2] or that are observed for anodically etched por-Si [5]. The por-Si was composed of two distinctly different regions. The upper layer was uniformly highly porous and was highly susceptible to cracking during drying. After etching for 3–7 hours, the surface of these samples looked shiny and was bronze in color while still in solution. If the sample was dried in a stream of Ar (or air), the sample immediately roughened and the color changed to yellow-green or brown. This upper layer can be removed by wiping with a kimwipe to reveal the lower layer. The reflectivities and colors of the upper and lower layers and how they change with angle are different.

By using critical point drying in CO_2 to avoid the damage produced by capillary forces [6], the shiny bronze appearance could be retained. SEM studies, see Fig. 1, confirmed that the por-Si film is composed of two layers. The upper layer was susceptible to cracking and exfoliation. Critical point drying reduced the extent of cracking and exfoliation but we have not yet been able to suppress them completely. This may indicate that some of the structural damage occurs either during etching or during the transfer of the sample from beaker to beaker during rinsing.

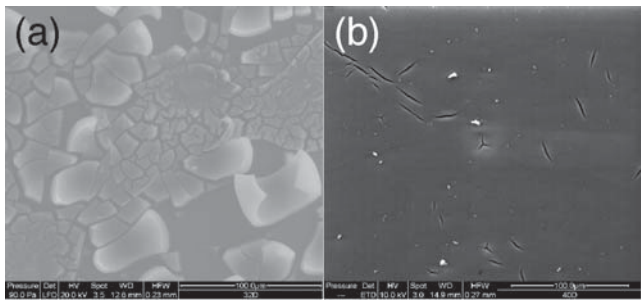

Figure 1 Scanning electron micrographs of stain etched samples after drying. (a) A sample dried in air, which exhibits exfoliation. (b) A sample produced by critical point drying that exhibits only cracking.

The curled exfoliated flakes allow us to measure the thickness of the upper layer. The flakes, and therefore the layer, is ~3 μm thick. We have not yet performed a systematic dependence of thickness versus etch time; however, cross-sectional SEM indicates that both the upper and lower layers can exhibit thicknesses in the range of 2–6 μm for etch times ≥3 h.

Cracking of porous films will result above a certain critical thickness h_c that depends on the surface energy of the liquid γ_L, the surface tension and bulk modulus of the solid γ_S and E_S, respectively, as well as the porosity ε and the pore radius r_p according to [6]

$$h_c = \left(\frac{r_p}{\gamma_L}\right)^2 E_S (1-\varepsilon)^3 \gamma_S , \quad (1)$$

where r_p is the pore radius, γ_L is the surface tension of the liquid (= 22.6 mN m^{-1} for ethanol), E_{Si} is the Young's modulus of bulk Si (162 × 10^9 N m^{-2}) [7] and γ_{Si} is the surface energy of Si (~1000 mN m^{-1}). Both the upper and the lower layers are uniform and display no structure in SE micrographs except for a few isolated pores with diameters of ~100 nm. This indicates that both layers are composed of micropores with diameters of <10 nm. For the 3 μm layer shown in Fig. 1 to exfoliate upon drying from methanol, the porosity has to exceed the critical porosity for cracking, which is $\varepsilon = 0.93$ for 10 nm pore diameter, $\varepsilon = 0.89$ for 5 nm pores, and $\varepsilon = 0.84$ for 3 nm pores (the size suggested from TEM images, see below). These values represent *minimum* porosities for the upper layer.

The lower layer did not exfoliate or crack and was mechanically more stable, which is consistent with a lower porosity. The lower layer more closely resembled por-Si made from $FeCl_3$ + HF etchants at short etching times. Dispersive X-ray spectroscopy (EDX) performed on samples that had been exposed to air for several days indicated that both layers were composed almost exclusively of Si with a small amount of F, perhaps from insufficient rinsing or diffusion into the por-Si, and O. The O content of the upper layer is greater, as would be expected for a higher surface area more porous solid, the surface of which has been partially oxidized by air exposure. No evidence for Fe incorporation in either layer is found. IR spectroscopy performed with an attenuated total reflectance (ATR) cell after a brief exposure of a freshly prepared sample to air confirms a predominantly hydrogen-terminated surface layer in the por-Si layer with little if any oxygen present.

Flakes from the upper layer were transferred to a TEM grid by mechanical abrasion after critical point drying. These images are still being analyzed but they reveal crystalline selective area diffraction patterns. In some regions we find patterns of linear lattice distortions that propagate into crystallites normal to the crystal facets. These are likely caused by stress and if we assume that the stress is induced by the presence of nanopores, the pore walls are ~2 nm or less and many of the pore openings are around 3 nm. A few much larger pores (around 50 nm) are also found. These results are consistent with SEM imaging in that generally (apart from drying induced cracks) the surfaces of both the upper and lower layers are smooth and featureless except for rare and isolated defect pores with openings between 50 nm and 100 nm.

3.3 Photoluminescence Etching for 3 h or more leads to much bluer PL than previously measured for ferric ion stain etchants used for ≤20 min [2]. The dual layers not only exhibit different structures, they also have distinctly different PL behavior as shown in Fig. 2. The upper layer emits bluer PL compared to the lower layer. The PL intensity and wavelength is quite uniform and highly robust. It does not diminish greatly in the yellow to red regions over the period of several days. The green region does become weaker as the film ages and oxidizes. The etch duration was varied over the period of 3–8 h. Etch duration affects both the PL intensity and the peak wavelength, with an optimum intensity occurring around 5–7 h. However we have not yet established an exact correlation between these two characteristics and the etch duration.

HF alone etching leads to a red peak (~645 nm), much like what is found for the lower layer. All yellow and green PL is associated with addition of H_2SO_4 and $HClO_4$, with little difference in PL peak wavelength regardless of which acid is used. While there is considerable scatter in the peak wavelength for the upper layer in the range of 560–615 nm, the addition of these acids consistently blueshifts the PL peak compared to HF alone. There is a correlation between adding more $FeCl_3 \cdot 6H_2O$ and a blue shift in the peak wavelength in HF : $HClO_4$.

Figures 3 and 4 demonstrate that the shape of the PL spectra change with excitation wavelength λ_{ex}, particularly if both layers are exposed. This indicates that the PLE spectrum will be a function of PL wavelength, as is shown in Figs. 5 and 6. The shift of the PL peak wavelength as the excitation wavelength is changed is complex when the upper layer is intact. When only the lower layer is irradiated,

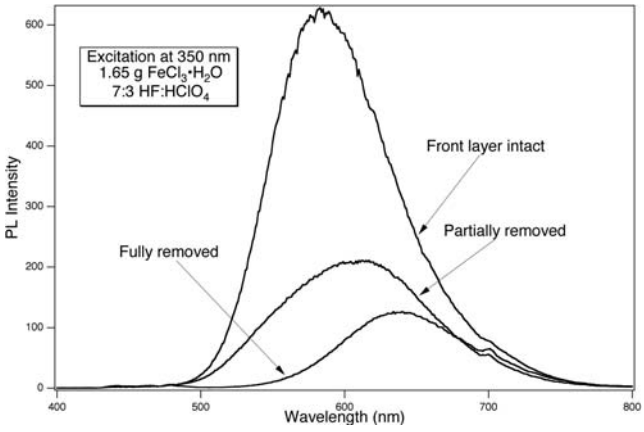

Figure 2 Photoluminescence excited by 350 nm light from por-Si layers with and without the highly porous upper layer.

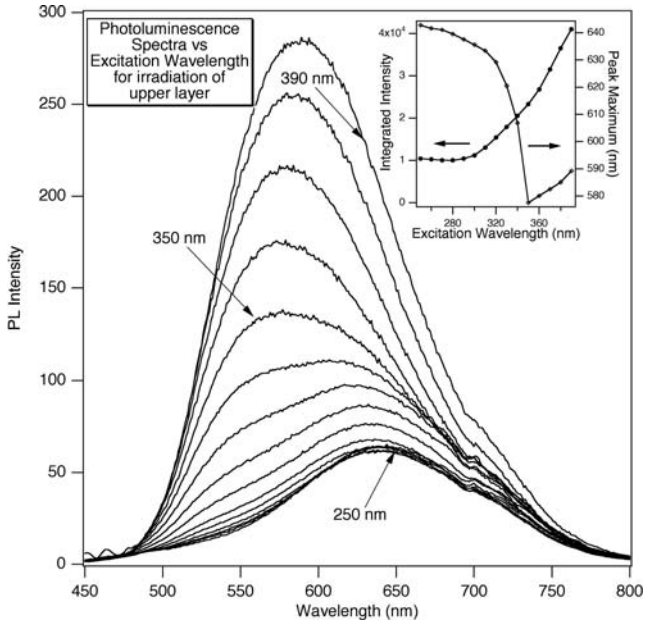

Figure 3 Photoluminescence spectra as a function of excitation wavelength ($250\ \text{nm} \le \lambda_{ex} \le 390\ \text{nm}$) recorded when the upper layer is intact. The inset shows how the peak wavelength and the integrated intensity change as a function of excitation wavelength.

the behavior is in line with expectation: the peak wavelength redshifts as the excitation wavelength increases.

The upper and lower layers clearly show different PL excitation spectra. In neither case does the excitation spectrum mirror the shape of the bulk silicon absorption coefficient. The upper layer PL excitation spectra, Fig. 5, all monotonically increase with increasing excitation wavelength, except for emission at 500 nm. Intensity is very low at this wavelength but it exhibits a weak resonance at 360 nm with a width of 90 nm (values obtained by fitting to a Gaussian function). The integrated PL intensity, inset Fig. 3, for the upper layer increases monotonically with increasing excitation wavelength.

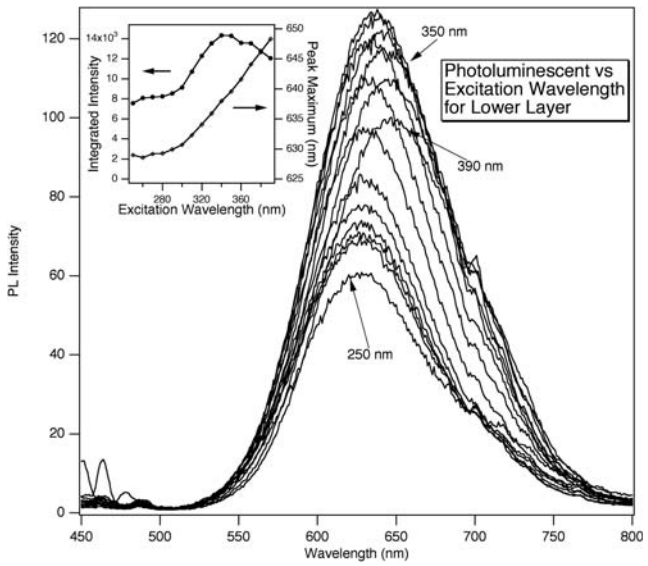

Figure 4 Photoluminescence spectra as a function of excitation wavelength ($250\ \text{nm} \le \lambda_{ex} \le 390\ \text{nm}$) recorded when the lower layer is exposed. The inset shows how the peak wavelength and the integrated intensity change as a function of excitation wavelength.

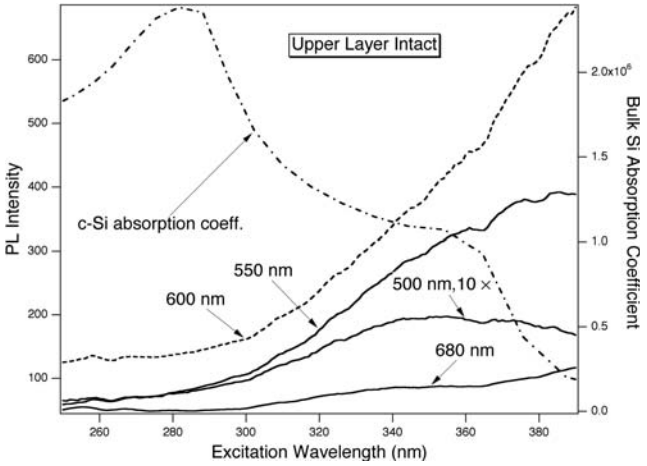

Figure 5 Photoluminescence excitation spectra recorded for emission at 500, 550, 600 and 680 nm with an intact upper layer.

The lower layer, Fig. 6, clearly shows a resonant feature at 340 nm with a 35 nm width for PL emission at 600 nm. At 680 nm, the PL intensity saturates and remains constant at and above 340 nm. For 550 nm excitation, the PL intensity decreases above 340 nm. The integrated PL intensity of the lower layer, inset Fig. 4, exhibits a resonant feature at 345 nm with a width of 50 nm. Because of the broad nature of these peaks, these values for the resonance positions are essentially equal.

Some of the variability in PL peak wavelength from sample to sample and why HF-alone etched samples are redder is explained by the dual layer structure and the fragility of the upper layer. The HF-alone etched samples

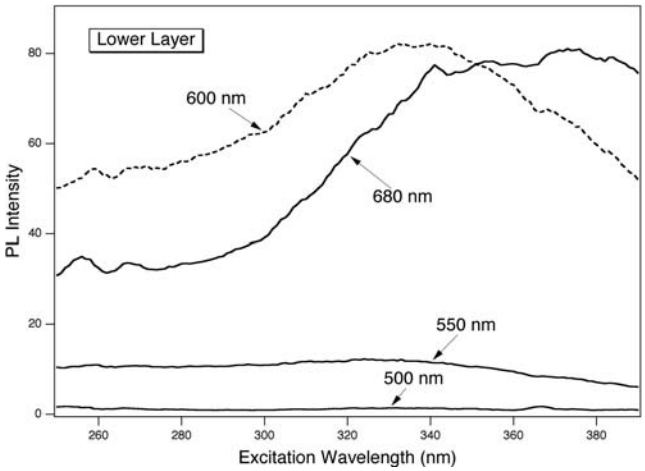

Figure 6 Photoluminescence excitation spectra recorded for emission at 500, 550, 600 and 680 nm without an upper layer.

only develop the lower porosity red-emitting layer. Depending on the extent of exfoliation or if by some other means some of the upper layer is removed, the PL spectrum will shift and broaden. It is important to note, however, that while the upper layer is fragile, its PL is not. Even after being removed from the substrate, the por-Si contained in the upper layer remains photoluminescent.

Clearly the upper and lower layers have different PL behaviors. Not only are the PL excitation spectra different, the peak wavelengths and their behaviors as a function of excitation wavelength are also different. The peak maximum of the lower layer changes monotonically from 629 nm to 648 nm as the excitation wavelength is changed from 250–390 nm, inset Fig. 4. Excitation of the upper layers exhibits two components, see Fig. 3. The blue component dominates the spectra with 350 nm $\leq \lambda_{ex} \leq$ 390 nm. Over this range its peak wavelength shifts from 577 nm to 589 nm. The red component dominates the spectra for 250 nm $\leq \lambda_{ex} \leq$ 310 nm. Over this range the peak shifts from 629 nm to 643 nm. Note that it is impossible to excite the upper layer exclusively without also exciting the lower layer as a result of the cracking and exfoliation that we always observe. This suggests that the red component may actually be due to excitation of the lower layer. The similarity in the wavelength of emission is consistent with this.

Several groups have measured the PLE spectra of anodically etched por-Si [8–11]. Mochizuki et al., Murayama et al. and Kanemitsu all found that the integrated intensity of the PL peak centered in the IR (at 730 nm, 775 nm and 730 nm, respectively) is essentially flat over a comparable range of λ_{ex}. Kanemitsu also found the same result for a peak centered at 630 nm. This behavior is unlike any we observe. On the other hand, Duan et al. found a broad resonant PLE feature centered at 340 nm for a PL peak centered at 610 nm. This behavior resembles that observed here for the lower layer.

4 Conclusion Stain etching in solutions composed not only of HF + Fe^{3+} but also concentrated $HClO_4$ or H_2SO_4 leads to porous silicon with a previously unreported structure when etching is performed for ≥3 hours. The highly photoluminescent por-Si exhibits a dual layer structure. The upper layer, with a thickness of ~3 μm, is brilliantly photoluminescent with a peak PL wavelength in the range of roughly 560–590 nm. With a porosity of at least 0.84, the upper layer is more porous than the lower layer and less mechanically stable. The lower layer has a redshifted PL spectrum that peaks in the range of 630–645 nm. The shape of the PL spectrum, particularly for the upper layer depends on the excitation wavelength. Photoluminescence excitation spectra demonstrate that the upper and lower layers are fundamentally different since they do not exhibit similar PLE spectra. Whereas the PL intensity in the green fades with time, the yellow to red PL is quite robust. Elemental analysis confirms that both layers do not contain any metal impurities; therefore, the differences must related to structural differences, which we infer to mean that they have different distributions of silicon nanocrystallites in their pore walls. Electron microscopy confirms that both layers exhibit highly uniform surface structures dominated by sub-10 nm pores. While there are a few pores in the range of 50–100 nm, estimates from TEM suggest that many of the pores are on the order of 3 nm in diameter with pore walls in the <2–5 nm range.

We speculate that the dual layer structure for etch times >3 h arises from two reactions occurring in the stain etchant. The first is conventional stain etching, which forms por-Si. The second is a much slower chemical reaction that gradually increases the porosity and blueshifts the PL spectrum, which is similar to the reaction suggested by Canham [12] in his original report of visible PL from high-porosity por-Si. Canham used a 6 h quiescent reaction in 40% aqueous HF to obtain visible PL in anodically etched por-Si.

Acknowledgements This work has been supported by West Chester University of Pennsylvania, the expert technical assistance of Frederick Monson, and the Center for Microanalysis Research and Training (CMIRT) at WCU. We also acknowledge Felix Goodson, Michael Moran and Anja Wellner for helpful discussions.

References

[1] K. W. Kolasinski, Curr. Opin. Solid State Mater. Sci. **9**, 73 (2005).
[2] M. Nahidi and K. W. Kolasinski, J. Electrochem. Soc. **153**, C19 (2006).
[3] K. W. Kolasinski, Phys. Chem. Chem. Phys. **5**, 1270 (2003).
[4] D. R. Turner, J. Electrochem. Soc. **107**, 810 (1960).
[5] A. G. Cullis, L. T. Canham, and P. D. J. Calcott, J. Appl. Phys. **82**, 909 (1997).
[6] D. Bellet and L. Canham, Adv. Mater. **10**, 487 (1998).
[7] D. Bellet, P. Lamagnére, A. Vincent, and Y. Bréchet, J. Appl. Phys. **80**, 3772 (1996).
[8] Y. Mochizuki, M. Mizuta, Y. Ochiai, S. Matsui, and N. Ohkubo, Phys. Rev. B **46**, 12353 (1992).
[9] K. Murayama, S. Miyazaki, and M. Hirose, Solid State Commun. **93**, 841 (1995).
[10] Y. Kanemitsu, Phys. Rep. **263**, 1 (1995).
[11] J. Q. Duan, G. Q. Yao, H. Z. Song, B. R. Zhang, L. Z. Zhang, and G. G. Qin, J. Appl. Phys. **78**, 478 (1995).
[12] L. T. Canham, Appl. Phys. Lett. **57**, 1046 (1990).

